



The effect of stress on point-defect diffusion in hcp metals and irradiation creep

C. H. WOO†

Department of Mechanical Engineering, Hong Kong Polytechnic University,
Kowloon, Hong Kong

and C. B. SO

Atomic Energy of Canada Ltd, Whiteshell Laboratories, Pinawa,
Manitoba R0E 1L0, Canada

[Received 7 April 1999 and accepted 11 November 1999]

ABSTRACT

Crystalline materials exposed to irradiation by high-energy particles produce defects such as lattice vacancies and interstitials. If the migration properties of the vacancy and interstitial are different, their annihilation behaviours at different sinks are biased. The resulting microstructure changes lead to macroscopic deformation. In hcp metals, anisotropic diffusion of the point defects is an intrinsic property related to the structure of the crystal lattice. The diffusional anisotropy is changed when a stress is applied to the crystal. The intrinsic anisotropy produces irradiation growth, while the stress-induced change in the diffusional anisotropy causes a deformation proportional to the applied stress, and contributes to irradiation creep. Irradiation creep due to the stress-induced change of the diffusion anisotropy has been investigated extensively in the cubic but not the hcp metals. In this paper, the elastodiffusion tensor of point defects in hcp metals is derived and applied to calculate the creep deformation by dislocations. The possibility that hydrostatic stress causes shear creep deformation is discussed.

§1. INTRODUCTION

One of the most important mechanisms of the irradiation-induced deformation of reactor materials is caused by the diffusional anisotropy difference (DAD) of vacancies and interstitials (Woo 1987a). Once generated under irradiation, these point defects will either recombine or undergo long-range migration and annihilate preferentially at different types of sink, such as dislocations and grain boundaries. DAD produces a large difference in their annihilation rates at sinks, producing a strong sink bias. This has a major effect on microstructure evolution and the concomitant macroscopic property changes under irradiation.

The anisotropic diffusion of point defects can either be intrinsic, that is due to the crystallographic anisotropy, or stress-induced. Hcp metals such as zirconium have a crystal structure that allows the simultaneous presence of both components. The intrinsic component contributes to irradiation growth (Woo and Gösele 1983).

† Email: mmchwoo@polyu.edu.hk.

The stress-induced component gives rise to a stress-induced preferred absorption (SIPA) effect that contributes to irradiation creep (Woo 1984, 1987a).

It is appropriate to point out that Savino (1977) and Dederichs and Schroeder (1978) were the first to suggest that the modification of the local anisotropy of the diffusion tensor, through the effect on the saddle-point configuration caused by an applied stress field, could lead to an effect on irradiation creep. This stress effect comes from the modification of the jump barrier caused by the coupling between the external stress field and the dislocation field, and the nonlinear dependence of the jump probability on the jump barrier. This coupling also produces a contribution to the SIPA effect (see also Woo and Savino (1983)), which Skinner and Woo (1984) later found to be only minor for straight dislocations, however. The major contribution (more than an order of magnitude larger) actually arises from the geometric inequivalence of the dislocation line direction in an anisotropic diffusion field, in a way that was pointed earlier by Woo and Gösele (1983). This justifies the neglect of the dislocation field in the formulation of the DAD effect (Woo 1988).

Extensive work on the theory of irradiation-induced growth due to DAD has been done on zirconium alloys since the initial work of Woo and Gösele (1983) (Woo 1988, 1998, Woo *et al.* 1992). Although SIPA due to DAD has also been studied extensively in cubic metals after its introduction by Woo (1984) (Woo 1995, Woo and Garner 1992, 1996, 1999, Woo *et al.* 1993), owing to the geometric complexity, a similar analysis in hcp metals has yet to be achieved. In this connection we note the numerical calculation of the irradiation-induced deformation in Zr (Fernández *et al.* 1994) due to stress-induced changes in the saddle-point energies. To link the theory with experiments more directly, we aim at a physically transparent relationship between the stress-dependent diffusion tensor and the final polycrystalline creep rate. To do this we follow an analytical route as in the case of cubic metals (Woo 1984). In this paper, we first derive the elastodiffusion tensor under an arbitrary applied stress for point defects in hcp metals. It is then used to evaluate the sink strengths of dislocations and the deformation rate induced by them.

§2. ELASTODIFFUSION TENSOR

Traditionally, the diffusivity tensor D_{km} of point defects, under a stress field is expressed in terms of the corresponding elastic strain field ε_{rl} (Flynn 1972, Dederichs and Schroeder 1978) as

$$D_{km} = D_{km}^0 + d_{kmrl}\varepsilon_{rl}, \quad (1)$$

where D_{km}^0 is the intrinsic stress-free diffusivity tensor and d_{kmrl} is the elastodiffusion tensor. This equation assumes that the strain ε_{rl} is small so that the contribution from the second term is much smaller than that of the first term. In the crystal's coordinate system†, D_{km}^0 can be written in matrix form

$$\mathbf{D}^0 = \begin{bmatrix} D_{\mathbf{a}}^0 & & \\ & D_{\mathbf{a}}^0 & \\ & & D_{\mathbf{c}}^0 \end{bmatrix} = D_{\mathbf{c}}^0 \begin{bmatrix} 1+q & & \\ & 1+q & \\ & & 1 \end{bmatrix} = D_{\mathbf{c}}^0 \bar{\mathbf{d}}. \quad (2)$$

† For hcp metals the crystal's coordinate system was chosen with the x and y axes to lie on the basal plane and the z axis coincided with the \mathbf{c} axis of the lattice. For cubic metals, the coordinate system coincided with that of the crystal lattice.

For hcp metals, D_a^0 and D_c^0 are the diffusion coefficients along the basal plane and c axis respectively. Unlike Woo (1988) who used the definition $p = (D_c^0/D_a^0)^{1/6}$ for the anisotropy factor, in this paper we use the definition $q = (D_a^0 - D_c^0)/D_c^0$. With this definition, $q = 0$ for isotropic materials such as cubic metals in which $D_a^0 = D_c^0$.

To simplify the mathematics, we follow Leibfried and Breuer (1978) and represent the strain ε_{rl} and stress σ_{rl} in terms of an orthonormal basis made up of the six eigentensors of the cubic symmetry $b_{rl}^{(\lambda)}$:

$$\begin{aligned} \sigma_{rl} &= \sigma^{(\lambda)} b_{rl}^{(\lambda)}, \\ \varepsilon_{rl} &= \varepsilon^{(\lambda)} b_{rl}^{(\lambda)}. \end{aligned} \tag{3}$$

(Einstein's summation notation is used here.) In this representation, any given stress σ_{rl} can be resolved into six independent components $\sigma^{(\lambda)}$. The same applies to the strain tensor. In Cartesian representation, $\mathbf{b}^{(\lambda)}$ can be written as

$$\begin{aligned} \mathbf{b}^{(1)} &= \frac{1}{6^{1/2}} \begin{bmatrix} 1 & 0 & 0 \\ 0 & 1 & 0 \\ 0 & 0 & -2 \end{bmatrix}, \quad \mathbf{b}^{(2)} = \frac{1}{2^{1/2}} \begin{bmatrix} 1 & 0 & 0 \\ 0 & -1 & 0 \\ 0 & 0 & 0 \end{bmatrix}, \quad \mathbf{b}^{(3)} = \frac{1}{2^{1/2}} \begin{bmatrix} 0 & 0 & 0 \\ 0 & 0 & 1 \\ 0 & 1 & 0 \end{bmatrix}, \\ \mathbf{b}^{(4)} &= \frac{1}{2^{1/2}} \begin{bmatrix} 0 & 0 & 1 \\ 0 & 0 & 0 \\ 1 & 0 & 0 \end{bmatrix}, \quad \mathbf{b}^{(5)} = \frac{1}{2^{1/2}} \begin{bmatrix} 0 & 1 & 0 \\ 1 & 0 & 0 \\ 0 & 0 & 0 \end{bmatrix}, \quad \mathbf{b}^{(6)} = \frac{1}{3^{1/2}} \begin{bmatrix} 1 & 0 & 0 \\ 0 & 1 & 0 \\ 0 & 0 & 1 \end{bmatrix}. \end{aligned} \tag{4}$$

Note that $\mathbf{b}^{(\lambda)}$ form an orthonormal complete set and their Cartesian components satisfy the condition $b_{rl}^{(\lambda)} b_{rl}^{(\lambda')} = \delta_{\lambda\lambda'}$. One can then expand the elastodiffusion tensor d_{kmrl} and the elastic compliance S_{kmrl} for either the cubic metals or the hcp metals as

$$\begin{aligned} d_{kmrl} &= d^{(\lambda,\lambda')} b_{km}^{(\lambda)} b_{rl}^{(\lambda')}, \\ S_{kmrl} &= S^{(\lambda,\lambda')} b_{km}^{(\lambda)} b_{rl}^{(\lambda')}. \end{aligned} \tag{5}$$

For cubic metals, the elements $d^{(\lambda,\lambda')}$ and $S^{(\lambda,\lambda')}$ are non-zero if and only if $\lambda = \lambda'$. For hcp metals, the same applies except for the cross-terms $d^{(6,1)}$, $d^{(1,6)}$, and $S^{(6,1)}$ and $S^{(1,6)}$ (Savino and Smetniansky-De Grande 1987). Furthermore, symmetry considerations also require $S^{(1,1)} = S^{(2,2)}$ and $S^{(3,3)} = S^{(4,4)} = S^{(5,5)}$ for cubic metals, while $S^{(2,2)} = S^{(5,5)}$ and $S^{(3,3)} = S^{(4,4)}$ for hcp metals. These symmetries also apply to $d^{(\lambda,\lambda')}$. With these relations, the diffusivity tensor given in equation (1) can be rewritten as

$$D_{km} = D_{km}^0 + d^{(\lambda,\beta)} b_{km}^{(\lambda)} \varepsilon^{(\beta)}. \tag{6}$$

Using equation (5) the strain field ε_{km} can be rewritten as

$$\begin{aligned} \varepsilon_{km} &= S^{(\beta,\lambda')} \sigma^{(\lambda')} b_{km}^{(\beta)} \\ \Rightarrow \varepsilon^{(\beta)} &= S^{(\beta,\lambda')} \sigma^{(\lambda')}. \end{aligned}$$

Substituting this into equation (6), the diffusivity tensor as a function of stress can be written as

$$D_{km} = D_{km}^0 (\bar{d}_{km} + \omega^{(\lambda,\lambda')} b_{km}^{(\lambda)} \sigma^{(\lambda')}), \tag{7}$$

where

$$\omega^{(\lambda,\lambda')} \equiv \frac{d^{(\lambda,\beta)}S^{(\beta,\lambda')}}{D_c^0}$$

are parameters that depend on the intrinsic properties of the metal, namely the elastic compliance and the dipole tensor and jump directions of the point defect (Dederichs and Schroeder 1978). To evaluate $\omega^{(\lambda,\lambda')}$, the values of $S^{(\lambda,\lambda')}$, $d^{(\lambda,\lambda')}$ and D_c^0 are needed.

§ 3. INTERNALLY PRESSURIZED TUBE

To gain some physical insight into the effect of stress on point-defect diffusion in hcp metals, we consider in this section the case of a zirconium tube, internally pressurized under a pressure p . The stress on each grain in the tube can be resolved, according to equation (3), into six components $\sigma^{(\lambda)}$ that depend on the orientation of the grain. For an arbitrary orientation, all elements in the diffusivity tensor are in general non-zero and have to be calculated accordingly. To concentrate on the underlying physics, we make the simplifying assumption that all grains are aligned with the **a** axis in the axial direction, and the **c** axis in the transverse direction.

Fischer and Renken (1964) measured the single crystal's elastic moduli of zirconium in terms of a stiffness tensor C_{kmrl} . Using the Voigt representation, its values are given in table 1. By inverting this stiffness tensor, one obtains the elastic compliance S_{kmrl} . This is converted to $S^{(\lambda,\lambda')}$ by equation (5). Their values are given in the table 2.

The components $d^{(\lambda,\lambda')}$ are a function of the dipole tensors of the point defects (vacancy and interstitial) and their jump vectors. There is little information on the dipole tensors for point defects in hcp metals. However, for the present purpose, these may be estimated from computer simulation of defect energetics using model interatomic potentials. Analytic expressions of $d^{(\lambda,\lambda')}$ for hcp metals as a function of

Table 1. Stiffness of Zr in Voigt notation.

C_{kmrl} (GPa)					
143.5	72.5	65.4			
72.5	143.5	65.4			
65.4	65.4	164.9			
			32.1		
				32.1	
					35.5

Table 2. $S^{(\lambda,\lambda')}$ of Zr [$\times 10^6$ MPa⁻¹].

$S^{(1.1)}$ (10 ⁶ MPa)	$S^{(2.2)}$ (10 ⁶ MPa)	$S^{(3.3)}$ (10 ⁶ MPa)	$S^{(6.6)}$ (10 ⁶ MPa)	$S^{(1.6)}$ (10 ⁶ MPa)	$S^{(6.1)}$ (10 ⁶ MPa)
10.58	14.09	15.58	3.49	0.25	0.25

Table 3. $D_{\mathbf{a}}^0$, $D_{\mathbf{c}}^0$ and $d^{(\lambda,\lambda')}$ of Zr at 560 K.

	Interstitial			Vacancy		
	P3C	P6C1	P6C2	P3C	P6C1	P6C2
$D_{\mathbf{a}}^0$ ($\text{m}^2 \text{s}^{-1}$)	6.7×10^{-9}	2.1×10^{-9}	19×10^{-9}	3.9×10^{-18}	4.0×10^{-19}	0.17×10^{-19}
$D_{\mathbf{c}}^0$ ($\text{m}^2 \text{s}^{-1}$)	5.4×10^{-9}	1.3×10^{-9}	11×10^{-9}	2.8×10^{-18}	2.9×10^{-19}	0.37×10^{-19}
$d^{(1,1)}$ ($\text{m}^2 \text{s}^{-1}$)	-3.2×10^{-7}	0.8×10^{-7}	19×10^{-7}	-1.7×10^{-16}	-2.6×10^{-17}	-0.26×10^{-17}
$d^{(2,2)}$ ($\text{m}^2 \text{s}^{-1}$)	2.0×10^{-7}	2.0×10^{-7}	6.3×10^{-7}	-2.0×10^{-16}	-2.3×10^{-17}	-0.11×10^{-17}
$d^{(3,3)}$ ($\text{m}^2 \text{s}^{-1}$)	0.7×10^{-7}	1.1×10^{-7}	25×10^{-7}	0.0	-0.2×10^{-17}	0.03×10^{-17}
$d^{(6,6)}$ ($\text{m}^2 \text{s}^{-1}$)	3.7×10^{-7}	0.3×10^{-7}	-24×10^{-7}	-7.9×10^{-16}	-3.9×10^{-17}	-0.46×10^{-17}
$d^{(6,1)}$ ($\text{m}^2 \text{s}^{-1}$)	-2.9×10^{-7}	2.4×10^{-7}	57×10^{-7}	-0.5×10^{-16}	0.1×10^{-17}	0.28×10^{-17}
$d^{(1,6)}$ ($\text{m}^2 \text{s}^{-1}$)	-0.8×10^{-7}	0.1×10^{-7}	-7.7×10^{-7}	-0.7×10^{-16}	-0.5×10^{-17}	0.22×10^{-17}

Table 4. q and $\omega^{(\lambda,\lambda')}$ of Zr at 560 K.

	Interstitial			Vacancy		
	P3C	P6C1	P6C2	P3C	P6C1	P6C2
q (MPa^{-1})	0.250	0.607	0.695	0.385	0.385	-0.534
$\omega^{(1,1)} \times 100$ (MPa^{-1})	-0.063	0.067	0.183	-0.064	-0.094	-0.073
$\omega^{(2,2)} \times 100$ (MPa^{-1})	0.052	0.209	0.081	-0.096	-0.110	-0.043
$\omega^{(3,3)} \times 100$ (MPa^{-1})	0.021	0.124	0.352	0.000	-0.010	0.014
$\omega^{(6,6)} \times 100$ (MPa^{-1})	0.023	0.014	-0.064	-0.097	-0.047	-0.042
$\omega^{(6,1)} \times 100$ (MPa^{-1})	-0.056	0.195	0.543	-0.026	0.002	0.077
$\omega^{(1,6)} \times 100$ (MPa^{-1})	-0.007	0.005	-0.020	-0.010	-0.008	0.019

the dipole tensor and the jump distances and directions have been derived by Savino and Smetniansky-De Grande (1987) and Smetniansky-de Grande *et al.* (1991). Using a jump frequency of 10^{13} , the values of $D_{\mathbf{a}}^0$, $D_{\mathbf{c}}^0$ and $d^{(\lambda,\lambda')}$ at 560 K are calculated with point-defect properties derived from three model interatomic potentials for Zr (denoted as P3C, P6C1 and P6C2 models due to Monti (1991)) and are listed in table 3. From these, q and $\omega^{(\lambda,\lambda')}$ are evaluated and listed in table 4. We note that these results were obtained assuming an ideal c/a ratio of 1.63 (instead of the measured value of 1.59) to conform to the interatomic potentials used to estimate the point-defect properties. It is obvious from table 4 that there is a large variation in the values of q and $\omega^{(\lambda,\lambda')}$ for the different model potentials. Nevertheless, they vary within the same order of magnitude.

Let the x and y axes be aligned with the axial and radial directions of the pressure tube respectively. Then the components of the external stress on the pressure tube are

$$\sigma^{(1)} = -\frac{3}{2} \times 6^{1/2} \frac{r}{t} p, \quad \sigma^{(2)} = \frac{1}{2^{3/2}} \frac{r}{t} p, \quad \sigma^{(6)} = \frac{3}{2} \times 3^{1/2} \frac{r}{t} p,$$

$$\sigma^{(3)} = \sigma^{(4)} = \sigma^{(5)} = 0.$$

Here r is the internal radius of the tube and t is the thickness of the tube wall. Using equation (7), the diffusivity tensor in the crystal's coordinate system reduces to

$$\mathbf{D} = D_{\mathbf{c}}^0 \begin{bmatrix} 1 + q - \left(\frac{\omega^{(1,1)}}{2} - \frac{\omega^{(2,2)}}{2} - \omega^{(6,6)} + \frac{\omega^{(6,1)}}{2^{1/2}} - \frac{\omega^{(1,6)}}{2^{1/2}} \right) \frac{r}{2t} p & 0 & 0 \\ 0 & 1 + q - \left(\frac{\omega^{(1,1)}}{2} + \frac{\omega^{(2,2)}}{2} - \omega^{(6,6)} + \frac{\omega^{(6,1)}}{2^{1/2}} - \frac{\omega^{(1,6)}}{2^{1/2}} \right) \frac{r}{2t} p & 0 \\ 0 & 0 & 1 + \left(\omega^{(1,1)} + \omega^{(6,6)} - \frac{\omega^{(6,1)}}{2^{1/2}} - 2^{1/2} \omega^{(1,6)} \right) \frac{r}{2t} p \end{bmatrix} \quad (8)$$

We note that the internal pressure induces an anisotropy in the diffusion on the basal plane, with $(D_{11} - D_{22})/D_{\mathbf{c}}^0$ equal to $\omega^{(2,2)}(r/2t)p$. This component exists for both the cubic and hcp metals.

Assuming the stress-induced contribution is much less than one, the anisotropy between the basal plane and the \mathbf{c} axis is also changed from q to

$$\frac{D_{11} - D_{33}}{D_{\mathbf{c}}^0} \approx q + (-3\omega^{(1,1)} + \omega^{(2,2)} + 3 \times 2^{1/2} \omega^{(1,6)}) \frac{r}{4t} p. \quad (9)$$

Note that the contribution from $\omega^{(2,2)}$ is equal to half the basal anisotropy. For cubic metals, $\omega^{(1,6)} = 0$ and $q = 0$, so that the hydrostatic contribution to the anisotropy disappears and the anisotropy reduces to $(-3\omega^{(1,1)} + \omega^{(2,2)})(r/4t)p$. However, for the hcp metals these contributions are non-zero.

In table 5, the contributions to the diffusional anisotropy are listed for a case with 10 MPa internal pressure. The second to fourth columns show the results for the interstitial while the fifth to seventh columns show those for the vacancy. The large variation in the results from one model potential to another indicates the sensitivity of diffusional anisotropy to the interatomic potential. A meaningful theoretical prediction of irradiation-induced deformation due to SIPA DAD cannot be made without an accurate interatomic potential. Since all three model potentials are pairwise in nature, they do not have the many-body contribution that is important in transition metals such as Zr. It is therefore questionable that any of these models is accurate enough for predictive purposes. However, several qualitative features may be deduced from the results.

Table 5. Contributions to the diffusion anisotropy in a pressure tube under internal pressure of 10 MPa ($r/t = 12.5$).

	Interstitial			Vacancy		
	P3C	P6C1	P6C2	P3C	P6C1	P6C2
q	0.250	0.606	0.695	0.385	0.385	-0.534
$-3\omega^{(1,1)}(r/4t)p$	0.059	-0.063	-0.169	0.060	0.088	0.069
$\omega^{(2,2)}(r/4t)p$	0.016	0.066	0.025	-0.030	-0.034	-0.013
$3 \times 2^{1/2} \omega^{(1,6)}(r/4t)p$	-0.009	0.007	-0.027	-0.013	-0.011	0.025

The contributions to the stress-induced anisotropy, shown in the last three rows of table 5, are all smaller than unity. Indeed, they are all smaller than the stress-free anisotropy factors q . This is consistent the original assumption used in equation (1). Furthermore, we note that all components have similar order of magnitudes. In contrast with the conventional belief that a hydrostatic applied stress does not produce significant shear deformation, it is not obvious that, in the present case, irradiation creep due to a hydrostatic applied stress can be ignored without careful consideration.

§4. IRRADIATION DEFORMATION DUE TO DIFFUSIONAL ANISOTROPY DIFFERENCE

During irradiation, DAD produces dislocation climb, and the concomitant deformation strain rate can be written (Woo 1988) as

$$\dot{\epsilon}_{mn} = \sum_{l \text{ class}} (Z_{li} \bar{D}_i^0 C_i - Z_{lv} \bar{D}_v^0 C_v) \rho_l \hat{b}_m^l \hat{b}_n^l. \quad (10)$$

Here the product $Z_{lj} \bar{D}_j^0 C_j$ is the diffusion current of j -type defects ($j = i$ for interstitial, $j = v$ for vacancy) into a unit segment of a dislocation. The dislocation is classified according to its Burgers vector \mathbf{b}^l and its class is denoted by l . ρ_l represents the dislocation density. $\bar{D}_j^0 = (\bar{D}_{xj}^0 \bar{D}_{yj}^0 \bar{D}_{zj}^0)^{1/3}$ is the mean stress-free diffusion coefficient of the j -type point defect in the material. C_j is the volume-averaged concentration of the j -type defect and Z_{lj} is the bias factor of dislocations of the l class. Under steady-state irradiation condition, C_i and C_v can be calculated in terms of the effective point-defect production rate G and the density of the sinks (Woo and Gösele 1983, Woo and Singh 1992). Then the steady-state deformation rate, calculated from equation (10), can be rewritten as

$$\dot{\epsilon}_{mn}^{(\beta)} = G \sum_l \left(\frac{k_{lj}^2}{k_{Ti}^2} - \frac{k_{lv}^2}{k_{Tv}^2} \right) \rho_l \hat{b}_m^l b_{mn}^{(\beta)}. \quad (11)$$

Here the strain-rate tensor is expanded in terms of the basis set $b_{mn}^{(\beta)}$ defined in the previous section. For the j -type point defects, k_{lj}^2 is the sink strength of l -class dislocation and is given by

$$k_{lj}^2 = \rho_l Z_{lj}, \quad (12)$$

and k_{Tj}^2 are the total sink strengths that include all types of sink. It is obvious from equation (10) that, to calculate the strain rate due to dislocation climb caused by DAD, Z_{lj} has to be evaluated.

4.1. Bias factor and creep contribution

Following Woo (1987a), we consider dislocations as an infinite straight cylindrical sink aligned with the z axis of the reference system (which will be referred to as the dislocation system). We neglect the dislocation strain field here, based on the results of Skinner and Woo (1984), that show that the large dependence of the dislocation bias on the line direction is not related to the strain field of the dislocation. In this section, we drop the reference to the defect type and to the dislocation class to simplify the notation. In this coordinate system, the diffusion of point defects to dislocations is reduced from a three-dimensional problem to a two-dimensional problem ($\partial C / \partial z = 0$ in the direction of the cylindrical axis). The bias factor Z , which

is identical with the reaction constant α of a dislocation used by Woo (1988) is given by

$$Z = \frac{2\pi}{\Omega} \frac{(\tilde{D}_x \tilde{D}_y)^{1/2}}{(D_c^0 D_a^0 D_a^0)^{1/3}} \frac{1}{\ln \{ [(4/\pi)(\tilde{D}_x \tilde{D}_y)^{1/2} \tau_{\text{eff}}]^{1/2} / r_0 \}}. \tag{13}$$

Here, \tilde{D}_x and \tilde{D}_y are the principal values of the diffusion tensor of the point defect in the x - y plane of the dislocation system. Since the logarithmic function is slowly varying, we ignore its variation with respect to the orientation of the dislocation in the following treatment (Woo 1987a). Then the problem of evaluating equation (13) is reduced to the calculation of $(\tilde{D}_x \tilde{D}_y)^{1/2}$ in the numerator.

We denote the angle made by the \mathbf{c} axis of the crystal with the dislocation line direction by λ (figure 1). The projection of the \mathbf{c} axis on to the x - y plane of the dislocation system has an angle ϕ with the y axis. Then $(\tilde{D}_x \tilde{D}_y)^{1/2}$ can be calculated (see appendix A) and the bias factor can be written as

$$Z \approx Z_0 \left\{ \begin{aligned} & (1 + q \cos^2 \lambda)^{1/2} \\ & + \frac{(1 + q \cos^2 \lambda)^{1/2}}{1 + q} \left[\left(1 - \frac{(3 + 2q) \sin^2 \lambda}{2(1 + q \cos^2 \lambda)} \right) \frac{\omega^{(1,1)}}{6^{1/2}} \right. \\ & \left. + \left(1 + \frac{q \sin^2 \lambda}{2(1 + q \cos^2 \lambda)} \right) \frac{\omega^{(6,1)}}{3^{1/2}} \right] \sigma^{(1)} \\ & + \frac{(1 + q \cos^2 \lambda)^{1/2}}{1 + q} \left[\left(1 - \frac{(3 + 2q) \sin^2 \lambda}{2(1 + q \cos^2 \lambda)} \right) \frac{\omega^{(1,6)}}{6^{1/2}} \right. \\ & \left. + \left(1 + \frac{q \sin^2 \lambda}{2(1 + q \cos^2 \lambda)} \right) \frac{\omega^{(6,6)}}{3^{1/2}} \right] \sigma^{(6)} \\ & + \frac{\sin^2 \lambda}{2^{3/2}(1 + q)(1 + q \cos^2 \lambda)^{1/2}} [\omega^{(2,2)} \sigma^{(2)} \cos(2\phi) - \omega^{(5,5)} \sigma^{(5)} \sin(2\phi)] \\ & - \frac{\sin(2\lambda)}{2^{3/2}(1 + q \cos^2 \lambda)^{1/2}} [\omega^{(3,3)} \sigma^{(3)} \cos \phi + \omega^{(4,4)} \sigma^{(4)} \sin \phi] \end{aligned} \right\}. \tag{14}$$

In this paper, we assume that dislocations are the dominant sinks. In appendix B, we show that equation (11) can be expressed as

$$\dot{\epsilon}^{(\beta)} = G \left\{ \dot{g}^{(\beta)} + \sum_{\beta'} K^{(\beta, \beta')} \sigma^{\beta'} \right\} \text{ for } \beta, \beta' = 1, 2, 3, 4, 5, 6. \tag{15}$$

The expressions for $\dot{g}^{(\beta)}$ and $K^{(\beta, \beta')}$ can also be found in appendix B. Here, $\dot{g}^{(\beta)}$ is the growth rate of the β mode of deformation and has the unit of reciprocal displacements per atom ($(\text{dpa})^{-1}$). The $K^{(\beta, \beta')}$ is the corresponding creep compliance of the β mode of deformation induced by the β' mode of stress and has the unit of $(\text{dpa} \times \text{GPa})^{-1}$.

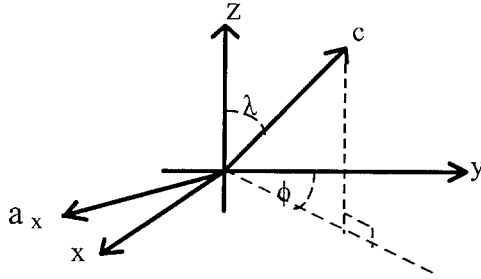


Figure 1. The coordinate system used in calculating point-defect diffusion into a infinitely long straight dislocation.

It is interesting to note from equation (15) that $K^{(\beta,6)}$ is in general non-zero, implying that a shear creep deformation can be caused by a hydrostatic stress in hcp metals. This will be further discussed in the next section.

4.2. Verification

Two special cases will be considered for the verification of equation (15). In the first case, we consider a single crystal with an isotropic distribution of dislocation line directions and Burgers vectors. In the absence of an applied stress, only irradiation growth is expected to occur and equation (15) reduces to

$$\begin{aligned} \dot{\epsilon}^{(1)} &= \frac{3G}{8 \times 6^{1/2}} \left[2 \left(\frac{(1 + q_i)^{3/2}}{q_i [(1 + q_i)^{1/2} + \Theta(q_i)]} - \frac{(1 + q_v)^{3/2}}{q_v [(1 + q_v)^{1/2} + \Theta(q_v)]} \right) - \left(\frac{1}{q_i} - \frac{1}{q_v} \right) \right], \\ \dot{\epsilon}^{(2)} = \dot{\epsilon}^{(3)} = \dot{\epsilon}^{(4)} = \dot{\epsilon}^{(5)} = \dot{\epsilon}^{(6)} &= 0, \end{aligned} \tag{16}$$

where

$$\Theta(q) = \frac{1}{2} \int_{-1}^1 \frac{dx}{(1 + qx^2)^{1/2}}$$

is calculated from appendix B, based on the assumption of isotropically distributed dislocations.

In Cartesian representation, we can write

$$\begin{aligned} \dot{\epsilon}_{11} = \dot{\epsilon}_{22} = \dot{\epsilon}^{(1)} b_{11}^{(1)} &= \frac{G}{16} \left[2 \left(\frac{(1 + q_i)^{3/2}}{q_i [(1 + q_i)^{1/2} + \Theta(q_i)]} - \frac{(1 + q_v)^{3/2}}{q_v [(1 + q_v)^{1/2} + \Theta(q_v)]} \right) \right. \\ &\quad \left. - \left(\frac{1}{q_i} - \frac{1}{q_v} \right) \right] \end{aligned} \tag{17}$$

and

$$\begin{aligned} \dot{\epsilon}_{33} = \dot{\epsilon}^{(1)} b_{33}^{(1)} &= \frac{-G}{8} \left[2 \left(\frac{(1 + q_i)^{3/2}}{q_i [(1 + q_i)^{1/2} + \Theta(q_i)]} - \frac{(1 + q_v)^{3/2}}{q_v [(1 + q_v)^{1/2} + \Theta(q_v)]} \right) \right. \\ &\quad \left. - \left(\frac{1}{q_i} - \frac{1}{q_v} \right) \right]. \end{aligned}$$

These results are identical with that derived by Woo (1984) assuming *a priori* isotropic diffusion in the stress-free crystal.

In the second case, we consider an uniaxial stress σ applied along the x axis of the lattice of a *cubic* metal with an isotropic dislocation structure. Then ω can be expressed in terms of the shear modulus μ and the saddle-point dipole tensor P_{ij} .

Equation (15) reduces to

$$\dot{\varepsilon}^{(3)} = \dot{\varepsilon}^{(4)} = \dot{\varepsilon}^{(5)} = \dot{\varepsilon}^{(6)} = 0,$$

$$\dot{\varepsilon}^{(\beta)} = \frac{-G}{40\mu kT} [P_i(1 - p_{i,1}) - P_v(1 - p_{v,1})]\sigma^{(\beta)} \quad \text{for } \beta = 1, 2, \quad (18)$$

where $P_i(P_v)$ is equal to a third of the trace of P_{ij} of interstitial (vacancy) and $p_{i,1}$ is one of the normalized eigenvalues of P_{ij} . In Cartesian representation,

$$\dot{\varepsilon}_{11} = \dot{\varepsilon}^{(1)}b_{11}^{(1)} + \dot{\varepsilon}^{(2)}b_{11}^{(2)} = \frac{-G}{60\mu kT} [P_i(1 - p_{i,1}) - P_v(1 - p_{v,1})]\sigma,$$

$$\dot{\varepsilon}_{22} = \dot{\varepsilon}_{33} = \dot{\varepsilon}^{(1)}b_{22}^{(1)} + \dot{\varepsilon}^{(2)}b_{22}^{(2)} = \frac{G}{120\mu kT} [P_i(1 - p_{i,1}) - P_v(1 - p_{v,1})]\sigma, \quad (19)$$

This result is also identical with that of Woo (1984).

§ 5. IRRADIATION CREEP CAUSED BY STRESS-INDUCED PREFERRED ABSORPTION DUE TO DIFFUSIONAL ANISOTROPY DIFFERENCE IN Zr ALLOYS

The rate of irradiation-induced deformation under the action of an applied stress due to DAD can be calculated using equation (15), provided that information on the elastodiffusion tensor, the texture and the microstructure is available. For the elastodiffusion tensor we use the results obtained earlier in this paper from point-defect properties calculated from model interatomic potentials.

The crystallographic misalignment of grains generates internal stresses in the material, which can only be properly accounted for with a polycrystalline model (Woo 1987b). However, our intention is to gain some qualitative information on the general behaviour of the deformation rate, and we restrict the present study to considering the single-crystal growth rate and creep compliance.

The microstructure of as-received pressure tube material has many classes of dislocation (Holt 1988). To take full account of all of them is very complicated and is not the intention of the present paper. Here, we shall simplify the problem by considering only a few key classes in order to follow an analytic route as much as possible. These are **a**-type dislocation loops on the prism planes, **c**-component loops on the basal planes and **c**-component dislocations also on the basal plane. Details of their Burgers vectors and line directions are as follows.

- (1) **a** loops have Burgers vector $\mathbf{b} = \frac{1}{3}\langle 11\bar{2}0 \rangle$ and lie on the prism planes. The line directions are $\langle 0001 \rangle$ ($\lambda = 0$), $\langle 1\bar{1}00 \rangle$ and $\langle 11\bar{2}0 \rangle$ ($\lambda = 90^\circ$).
- (2) **c'**-component loops have Burgers vector $\mathbf{b} = \frac{1}{6}\langle 20\bar{2}3 \rangle$ and lie on the basal planes. The line directions are $\langle 1\bar{1}00 \rangle$ and $\langle 11\bar{2}0 \rangle$ ($\lambda = 90^\circ$).
- (3) **c**-loops have the Burgers vector $\mathbf{b} = \langle 0001 \rangle$ and lie on the basal plane. The line directions are $\langle 1\bar{1}00 \rangle$ and $\langle 11\bar{2}0 \rangle$ ($\lambda = 90^\circ$).

Their respective line densities are denoted by ρ_a , $\rho_{c'}$ and ρ_c , which we express as fractions of the total dislocation density:

$$\rho_{\mathbf{a}} + \rho_{\mathbf{c}} + \rho_{\mathbf{c}'} = 1.$$

From these, the single-crystal growth rate and creep compliance can be derived from equation (B 3) of appendix B, assuming that the line density is not a function of line directions:

$$\begin{aligned}\dot{\varepsilon}^{(1)} &= G(\dot{g}^{(1)} + K^{(1,1)}\sigma^{(1)} + K^{(1,6)}\sigma^{(6)}), \\ \dot{\varepsilon}^{(2)} &= GK^{(2,2)}\sigma^{(2)}, \\ \dot{\varepsilon}^{(5)} &= GK^{(2,2)}\sigma^{(5)}, \\ \dot{\varepsilon}^{(3)} &= \dot{\varepsilon}^{(4)} = \dot{\varepsilon}^{(6)} = 0,\end{aligned}\tag{20}$$

where

$$\begin{aligned}\dot{g}^{(1)} &= \frac{6^{1/2}\rho_{\mathbf{a}}(\rho_{\mathbf{c}} + B\rho_{\mathbf{c}'})}{4} \frac{(1 + q_{\mathbf{i}})^{1/2} - (1 + q_{\mathbf{v}})^{1/2}}{\{1 + \frac{1}{2}\rho_{\mathbf{a}}[(1 + q_{\mathbf{i}})^{1/2} - 1]\}\{1 + \frac{1}{2}\rho_{\mathbf{a}}[(1 + q_{\mathbf{v}})^{1/2} - 1]\}}, \\ K^{(1,\beta')} &= \frac{\rho_{\mathbf{a}}(\rho_{\mathbf{c}} + B\rho_{\mathbf{c}'})}{8} \left(\frac{(3 + 2q_{\mathbf{i}})\omega_{\mathbf{i}}^{(1,\beta')} - 2^{1/2}q_{\mathbf{i}}\omega_{\mathbf{i}}^{(6,\beta')}}{\{1 + \frac{1}{2}\rho_{\mathbf{a}}[(1 + q_{\mathbf{i}})^{1/2} - 1]\}^2(1 + q_{\mathbf{i}})^{1/2}} \right. \\ &\quad \left. - \frac{(3 + 2q_{\mathbf{v}})\omega_{\mathbf{v}}^{(1,\beta')} - 2^{1/2}q_{\mathbf{v}}\omega_{\mathbf{v}}^{(6,\beta')}}{\{1 + \frac{1}{2}\rho_{\mathbf{a}}[(1 + q_{\mathbf{v}})^{1/2} - 1]\}^2(1 + q_{\mathbf{v}})^{1/2}} \right), \\ K^{(2,2)} &= K^{(5,5)} = \frac{\rho_{\mathbf{a}}}{16} \left(\frac{\omega_{\mathbf{i}}^{(2,2)}}{(1 + q_{\mathbf{i}})\{1 + \frac{1}{2}\rho_{\mathbf{a}}[(1 + q_{\mathbf{i}})^{1/2} - 1]\}} \right. \\ &\quad \left. - \frac{\omega_{\mathbf{v}}^{(2,2)}}{(1 + q_{\mathbf{v}})\{1 + \frac{1}{2}\rho_{\mathbf{a}}[(1 + q_{\mathbf{v}})^{1/2} - 1]\}} \right), \\ B &= \left(\frac{c^2}{4a^2} \right) / \left(\frac{1}{3} + \frac{c^2}{4a^2} \right) \approx 0.657 \text{ for Zr.}\end{aligned}\tag{21}$$

In equation (21), $\beta' = 1$ or 6. Because of the crystal symmetry, the growth rate has only one mode of deformation, namely the pyramidal mode. There are usually very few \mathbf{c} -type dislocations in the as-received materials, until they are irradiated. Therefore we can assume that $\rho_{\mathbf{c}} \approx 0$ in this case. Using the diffusion tensors obtained from the three interatomic potentials mentioned above, the results are shown in figure 2 for three different temperatures: 300, 450 and 560 K. Also shown is the irradiation growth rate calculated from the diffusional anisotropy determined by fitting to loop growth rates measured by high-voltage electron microscopy (Woo 1998). It is clear that the variability between the calculated results from the different potentials is large. Only the result obtained from the P6C2 potential at high temperatures can be compared with the experiment. The other two models predict contraction when the experiment measures elongation. This large variability of the predictions indicates that interatomic potentials used here are not accurate enough to give the correct intrinsic anisotropy q . This can be understood, because the potentials are pairwise in nature and are questionable in representing the true interatomic interactions of transition metals, as we have mentioned.

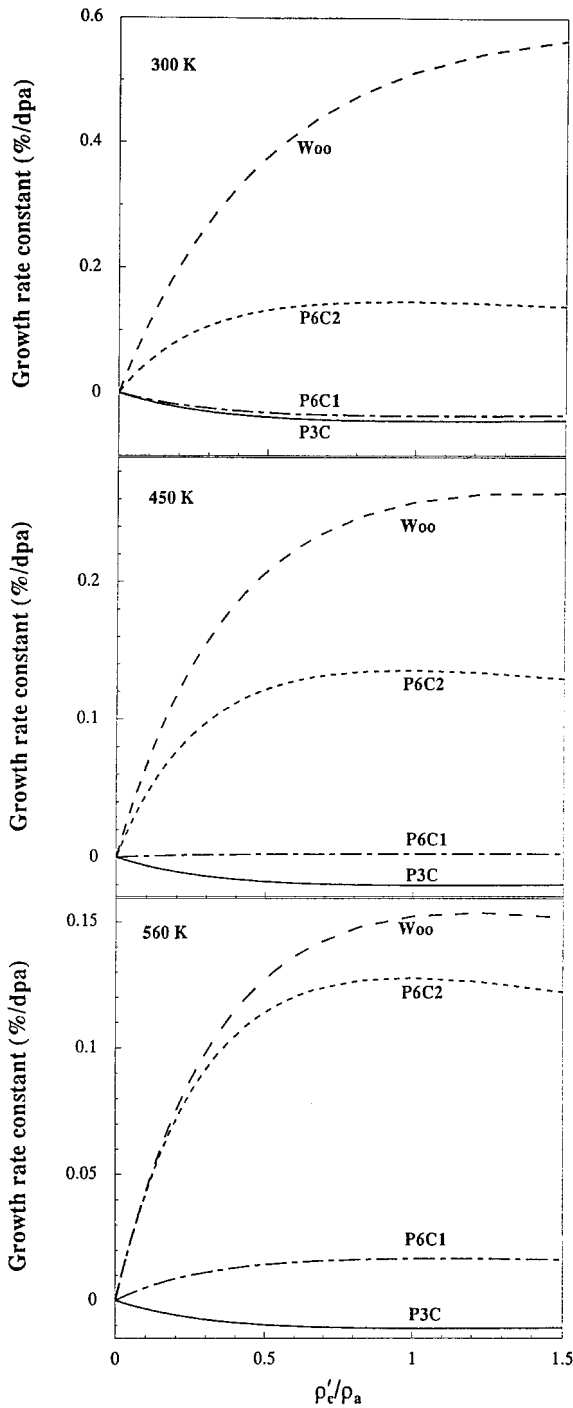


Figure 2. Calculated single-crystal irradiation growth rate $g^{(1)}$ from three model interatomic potentials, in comparison with those calculated from diffusional anisotropy determined by fitting to loop growth rates measured by high-voltage electron microscopy. The % in the unit of the vertical axis means that the creep and growth rates have been multiplied by a factor of 100.

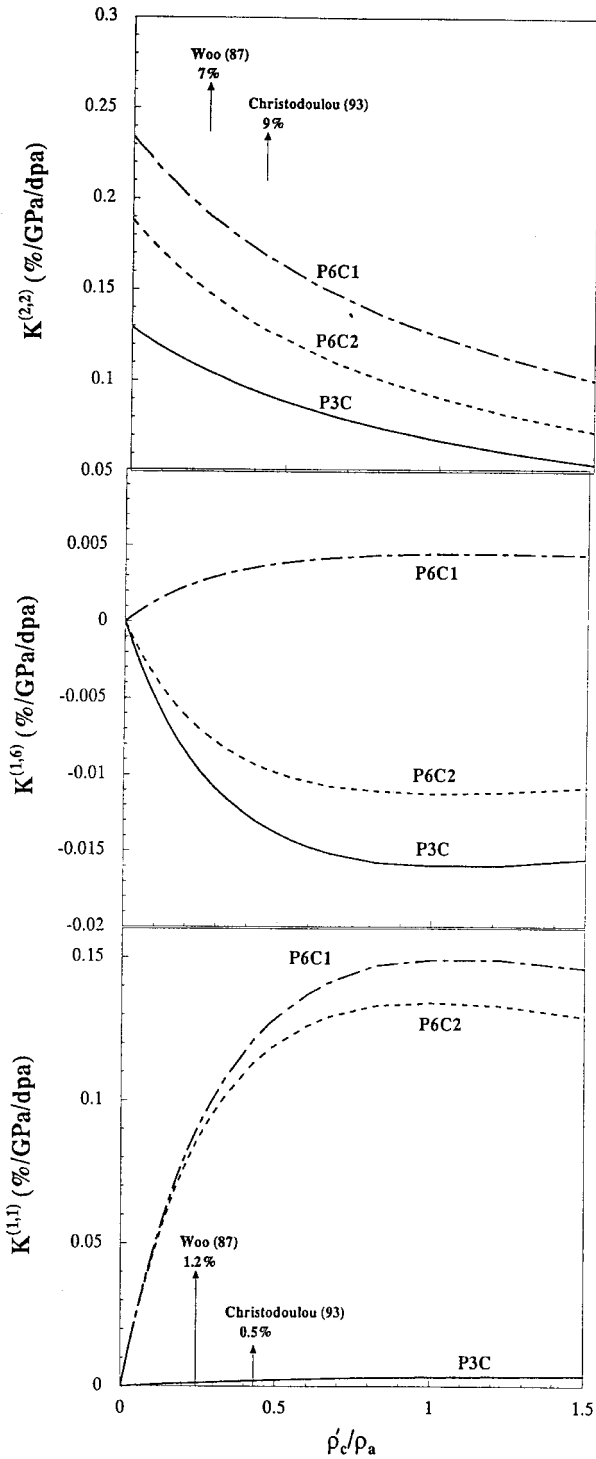


Figure 3. Calculated single-crystal irradiation creep compliance rates from three model interatomic potentials, in comparison with those determined from experimental creep data via polycrystalline models (Woo 1987b, Christodoulou *et al.* 1993).

Figure 3 shows the calculated creep compliances using the three model potentials. They are underestimated by an order of magnitude when compared with the experimental data (Woo 1987b, 1998, Christodoulou *et al.* 1993). This could be either the result of the improper interatomic potentials or because the controlling mechanism of creep in pressure tube material is not SIPA DAD. The prismatic creep mode $K^{(2,2)}$ makes the largest contribution. This agrees with experiment. The pyramidal creep compliance induced by the hydrostatic stress component $K^{(1,1)}$ is about 9% of that induced by the pyramidal stress component $K^{(1,1)}$. Therefore, if the pyramidal component of the stress is about the same as that of the hydrostatic component, the contribution from $K^{(1,6)}$ to $\dot{\epsilon}^{(1)}$ can be ignored. However, for an arbitrarily applied stress, it must be included because the hydrostatic component of the stress may become the dominant component. For example, a pure hydrostatic stress induces a pyramidal shear rate in Zr due to $K^{(1,6)}$. This does not apply to cubic metals.

§6. SUMMARY AND CONCLUSIONS

The elastodiffusion tensor of point defects was derived for the hcp metals. The stress-induced diffusional anisotropy was investigated. It was found that hydrostatic stress might have a substantial effect in altering the diffusion behaviour of point defects in pressure tube.

The reaction constant, sink strength and the strain rate due to SIPA DAD on dislocations were also evaluated. The results were verified against cases with known solution. The growth rate and creep compliances of a single crystal of Zr were calculated using dipole tensors obtained from three different interatomic potentials. The results show that four stress components contribute to creep. The prismatic components have the largest contribution to creep. The hydrostatic stress component, if large, can also contribute substantially to creep. This contribution exists only for hcp materials and not in cubic materials.

ACKNOWLEDGEMENTS

The authors wish to acknowledge funding support from Hong Kong Research Grant Council (PolyU 5123/98E) (C.H.W.) and CANDU Owners Group (C.B.S.).

A P P E N D I X A

CALCULATION OF $(\tilde{D}_x \tilde{D}_y)^{1/2}$ AND Z

The elastodiffusion tensor, in an arbitrary coordinate system, is given by equation (7). By choosing the z axis (see figure 1) of the reference system, that is the dislocation system, to align with the dislocation-line direction, the diffusion of point defects to an infinitely long dislocation is reduced from a three-dimensional problem to a two-dimensional problem ($\partial C / \partial z = 0$). Furthermore, since the stress-free diffusion tensor is isotropic in the basal plane, the choice of basal axes with respect to the dislocation system is arbitrary. Therefore we can choose one of the basal axes to lie on the x - y plane of the dislocation-system. In this coordinate system, ψ equals zero and the non-zero x - y components of the matrix functions reduce to

$$\begin{aligned}
 \bar{\mathbf{d}} &= \left\{ \begin{array}{c} 1+q \\ 1+q \cos^2 \lambda \end{array} \right\}, \quad \mathbf{b}^{(1)} = \frac{1}{6^{1/2}} \left\{ \begin{array}{c} 1 \\ 1-3 \sin^2 \lambda \end{array} \right\}, \\
 \mathbf{b}^{(6)} &= \frac{1}{3^{1/2}} \left\{ \begin{array}{c} 1 \\ 1 \end{array} \right\}, \\
 \mathbf{b}^{(2)} &= \frac{1}{2^{1/2}} \left\{ \begin{array}{cc} \cos(2\phi) & \sin(2\phi) \cos \lambda \\ \sin(2\phi) \cos \lambda & -\cos^2 \lambda \cos(2\phi) \end{array} \right\}, \\
 \mathbf{b}^{(5)} &= \frac{1}{2^{1/2}} \left\{ \begin{array}{cc} -\sin(2\phi) & \cos(2\phi) \cos \lambda \\ \cos(2\phi) \cos \lambda & \cos^2 \lambda \sin(2\phi) \end{array} \right\}, \\
 \mathbf{b}^{(3)} &= \frac{1}{2^{1/2}} \left\{ \begin{array}{cc} \sin \phi \sin \lambda & \\ \sin \phi \cos \lambda & -\cos \phi \sin(2\lambda) \end{array} \right\}, \\
 \mathbf{b}^{(4)} &= \frac{1}{2^{1/2}} \left\{ \begin{array}{cc} & -\cos \phi \sin \lambda \\ -\cos \phi \sin \lambda & -\sin \phi \sin(2\lambda) \end{array} \right\}.
 \end{aligned} \tag{A 1}$$

Then the elastodiffusion tensor becomes

$$\frac{D_{km}}{D_e^0} = \left\{ \begin{array}{cc} (1+q) + \left(\frac{w^{(1,1)}}{6^{1/2}} + \frac{\omega^{(6,1)}}{3^{1/2}} \right) \sigma^{(1)} & \vdots \\ + \left(\frac{\omega^{(1,6)}}{6^{1/2}} + \frac{\omega^{(6,6)}}{3^{1/2}} \right) \sigma^{(6)} & \left(\frac{\omega^{(2,2)}}{2^{1/2}} \sigma^{(2)} \sin(2\phi) + \frac{\omega^{(5,5)}}{2^{1/2}} \sigma^{(5)} \cos(2\phi) \right) \cos \lambda \\ + \frac{\omega^{(2,2)}}{2^{1/2}} \sigma^{(2)} \cos(2\phi) & + \left(\frac{\omega^{(3,3)}}{2^{1/2}} \sigma^{(3)} \sin \phi - \frac{\omega^{(4,4)}}{2^{1/2}} \sigma^{(4)} \cos \phi \right) \sin \lambda \\ - \frac{\omega^{(5,5)}}{2^{1/2}} \sigma^{(5)} \sin(2\phi) & \\ \hline \left(\frac{\omega^{(2,2)}}{2^{1/2}} \sigma^{(2)} \sin(2\phi) \right. & 1 + \left[q + \left(\frac{\omega^{(1,1)}}{6^{1/2}} + \frac{\omega^{(6,1)}}{3^{1/2}} \right) \sigma^{(1)} + \left(\frac{\omega^{(1,6)}}{6^{1/2}} + \frac{\omega^{(6,6)}}{3^{1/2}} \right) \sigma^{(6)} \right. \\ \left. + \frac{\omega^{(5,5)}}{2^{1/2}} \sigma^{(5)} \cos(2\phi) \right) \cos \lambda & \left. - \frac{\omega^{(2,2)}}{2^{1/2}} \sigma^{(2)} \cos(2\phi) + \frac{\omega^{(5,5)}}{2^{1/2}} \sigma^{(5)} \sin(2\phi) \right] \cos^2 \lambda \\ + \left(\frac{\omega^{(3,3)}}{2^{1/2}} \sigma^{(3)} \sin \phi \right. & \left. + \left[\left(\frac{\omega^{(6,1)}}{3^{1/2}} - \frac{2\omega^{(1,1)}}{6^{1/2}} \right) \sigma^{(1)} + \left(\frac{\omega^{(6,6)}}{3^{1/2}} - \frac{2\omega^{(1,6)}}{6^{1/2}} \right) \sigma^{(6)} \right] \sin^2 \lambda \right. \\ \left. - \frac{\omega^{(4,4)}}{2^{1/2}} \sigma^{(4)} \cos \phi \right) \sin \lambda & \left. - \left(\frac{\omega^{(3,3)}}{2^{1/2}} \sigma^{(3)} \cos \phi + \frac{\omega^{(4,4)}}{2^{1/2}} \sigma^{(4)} \sin \phi \right) \sin(2\lambda) \right\}
 \end{array} \tag{A 2}$$

The eigenvalues of this matrix becomes the principal values of the diffusion tensor, \tilde{D}_x and \tilde{D}_y . However, we do not need to solve for \tilde{D}_x and \tilde{D}_y independently, because $(\tilde{D}_x \tilde{D}_y)^{1/2}$ can be calculated from equation (A 2) quite readily †:

† If x_1 and x_2 are the roots of the quadratic equation $x^2 + bx + c = 0$, then $x_1 x_2 = c$.

$$\begin{aligned}
\frac{(\tilde{D}_x \tilde{D}_y)^{1/2}}{D_c^0} &\approx \left\{ (1+q \cos^2 \lambda) \left[(1+q) + \left(\frac{\omega^{(1,1)}}{6^{1/2}} + \frac{\omega^{(6,1)}}{3^{1/2}} \right) \rho^{(1)} + \left(\frac{\omega^{(1,6)}}{6^{1/2}} + \frac{\omega^{(6,6)}}{3^{1/2}} \right) \rho^{(6)} \right] \right. \\
&+ \frac{1+q \cos^2 \lambda}{2^{1/2}} [\omega^{(2,2)} \sigma^{(2)} \cos(2\phi) - \omega^{(5,5)} \sigma^{(5)} \sin(2\phi)] \\
&+ (1+q) \left[\left(\frac{\omega^{(1,1)}}{6^{1/2}} + \frac{\omega^{(6,1)}}{3^{1/2}} \right) \rho^{(1)} + \left(\frac{\omega^{(1,6)}}{6^{1/2}} + \frac{\omega^{(6,6)}}{3^{1/2}} \right) \rho^{(6)} \right] \cos^2 \lambda \\
&- \frac{1+q}{2^{1/2}} [\omega^{(2,2)} \sigma^{(2)} \cos(2\phi) - \omega^{(5,5)} \sigma^{(5)} \sin(2\phi)] \cos^2 \lambda \\
&+ (1+q) \left[\left(\frac{\omega^{(6,1)}}{3^{1/2}} - \frac{2\omega^{(1,1)}}{6^{1/2}} \right) \rho^{(1)} + \left(\frac{\omega^{(6,6)}}{3^{1/2}} - \frac{2\omega^{(1,6)}}{6^{1/2}} \right) \rho^{(6)} \right] \sin^2 \lambda \\
&\left. - \frac{1+q}{2^{1/2}} (\omega^{(3,3)} \sigma^{(3)} \cos \phi + \omega^{(4,4)} \sigma^{(4)} \sin \phi) \sin(2\lambda) \right\}^{1/2} \\
&= \left\{ (1+q)(1+q \cos^2 \lambda) + (1+q) \sin^2 \lambda \left[\left(\frac{\omega^{(6,1)}}{3^{1/2}} - \frac{2\omega^{(1,1)}}{6^{1/2}} \right) \sigma^{(1)} \right. \right. \\
&+ \left. \left. \left(\frac{\omega^{(6,6)}}{3^{1/2}} - \frac{2\omega^{(1,6)}}{6^{1/2}} \right) \rho^{(6)} \right] \right. \\
&+ [2(1+q \cos^2 \lambda) - \sin^2 \lambda] \left[\left(\frac{\omega^{(1,1)}}{6^{1/2}} + \frac{\omega^{(6,1)}}{3^{1/2}} \right) \rho^{(1)} + \left(\frac{\omega^{(1,6)}}{6^{1/2}} + \frac{\omega^{(6,6)}}{3^{1/2}} \right) \rho^{(6)} \right] \\
&+ [\omega^{(2,2)} \sigma^{(2)} \cos(2\phi) - \omega^{(5,5)} \sigma^{(5)} \sin(2\phi)] \frac{\sin^2 \lambda}{2^{1/2}} \\
&\left. - (\omega^{(3,3)} \sigma^{(3)} \cos \phi + \omega^{(4,4)} \sigma^{(4)} \sin \phi) \frac{(1+q) \sin(2\lambda)}{2^{1/2}} \right\}^{1/2}. \tag{A 3}
\end{aligned}$$

Assuming that the contribution from the stress is small compared with the stress-free components, we retain terms only to the first order in stress:

$$\begin{aligned}
\frac{(\tilde{D}_x \tilde{D}_y)^{1/2}}{D_c^0} &\approx (1+q)^{1/2} (1+q \cos^2 \lambda)^{1/2} \left\{ 1 + \frac{\sin^2 \lambda}{2(1+q \cos^2 \lambda)} \left[\left(\frac{\omega^{(6,1)}}{3^{1/2}} - \frac{2\omega^{(1,1)}}{6^{1/2}} \right) \sigma^{(1)} \right. \right. \\
&+ \left. \left. \left(\frac{\omega^{(6,6)}}{3^{1/2}} - \frac{2\omega^{(1,6)}}{6^{1/2}} \right) \rho^{(6)} \right] \right. \\
&+ \frac{2(1+q \cos^2 \lambda) - \sin^2 \lambda}{2(1+q)(1+q \cos^2 \lambda)} \left[\left(\frac{\omega^{(1,1)}}{6^{1/2}} + \frac{\omega^{(6,1)}}{3^{1/2}} \right) \rho^{(1)} + \left(\frac{\omega^{(1,6)}}{6^{1/2}} + \frac{\omega^{(6,6)}}{3^{1/2}} \right) \rho^{(6)} \right] \\
&+ \frac{\sin^2 \lambda}{2^{3/2}(1+q)(1+q \cos^2 \lambda)} [\omega^{(2,2)} \sigma^{(2)} \cos(2\phi) - \omega^{(5,5)} \sigma^{(5)} \sin(2\phi)]
\end{aligned}$$

$$\begin{aligned}
 & - \frac{\sin(2\lambda)}{2^{3/2}(1+q\cos^2\lambda)} \left(\omega^{(3,3)}\sigma^{(3)}\cos\phi + \omega^{(4,4)}\sigma^{(4)}\sin\phi \right) \Big\} \\
 \approx & (1+q)^{1/2} \left\{ (1+q\cos^2\lambda)^{1/2} + \frac{(1+q\cos^2\lambda)^{1/2}}{1+q} \left[\left(1 - \frac{(3+2q)\sin^2\lambda}{2(1+q\cos^2\lambda)} \right) \right. \right. \\
 \times & \left. \frac{\omega^{(1,1)}}{6^{1/2}} + \left(1 + \frac{q\sin^2\lambda}{2(1+q\cos^2\lambda)} \right) \frac{\omega^{(6,1)}}{3^{1/2}} \right] \sigma^{(1)} \\
 + & \frac{(1+q\cos^2\lambda)^{1/2}}{1+q} \left[\left(1 - \frac{(3+2q)\sin^2\lambda}{2(1+q\cos^2\lambda)} \right) \frac{\omega^{(1,6)}}{6^{1/2}} \right. \\
 + & \left. \left(1 + \frac{q\sin^2\lambda}{2(1+q\cos^2\lambda)} \right) \frac{\omega^{(6,6)}}{3^{1/2}} \right] \sigma^{(6)} \\
 + & \frac{\sin^2\lambda}{2^{3/2}(1+q)(1+q\cos^2\lambda)^{1/2}} \left[\omega^{(2,2)}\sigma^{(2)}\cos(2\phi) - \omega^{(5,5)}\sigma^{(5)}\sin(2\phi) \right] \\
 - & \left. \frac{\sin(2\lambda)}{2^{3/2}(1+q\cos^2\lambda)^{1/2}} \left[\omega^{(3,3)}\sigma^{(3)}\cos\phi + \omega^{(4,4)}\sigma^{(4)}\sin\phi \right] \right\}. \tag{A 4}
 \end{aligned}$$

Then substitute this into equation (13) to yield the bias factor in equation (14), in which

$$Z_0 = \frac{2\pi}{\Omega} \left(\frac{D_c^0}{D_a^0} \right)^{2/3} \frac{(1+q)^{1/2}}{\ln \{ [(4/\pi)(\tilde{D}_x\tilde{D}_y)^{1/2}\tau_{\text{eff}}]^{1/2}/r_0 \}} \approx \frac{2\pi}{\Omega} \frac{1}{(1+q)^{1/6}} \frac{1}{\ln(r_\infty/r_0) - 0.57}$$

is the intrinsic bias factor which is independent of stress and orientation of the dislocation. Here we have used $r_\infty = [4(\tilde{D}_x\tilde{D}_y)^{1/2}\tau_{\text{eff}}]^{1/2}$ (Woo 1988).

APPENDIX B

CALCULATION OF THE STRAIN RATE

We assume the dislocation is the dominant sink such that

$$k_T^2 \approx \sum_{l\text{class}} k_l^2 = \sum_{l\text{class}} \rho_l Z_l.$$

Here we drop the reference to the defect type for simplification. Then the calculation of the strain rate from equation (11) is reduced to the calculation of the terms $N_d Z_0 \sum_{l\text{class}} k_l^2$ and $\sum_{l\text{class}} k_l^2 \hat{b}_m^l \hat{b}_n^l b_{mn}^{(\beta)}$. Using equations (12) and (14),

$$\begin{aligned}
 k_{\text{T}}^2 \approx N_{\text{d}} Z_0 \tilde{Q} & \left[1 + \left([1 - (3 + 2q)\tilde{\psi}] \frac{\omega^{(1,1)}}{6^{1/2}} + (1 + q\tilde{\psi}) \frac{\omega^{(6,1)}}{3^{1/2}} \right) \frac{\sigma^{(1)}}{1 + q} \right. \\
 & + \left([1 - (3 + 2q)\tilde{\psi}] \frac{\omega^{(1,6)}}{6^{1/2}} + (1 + q\tilde{\psi}) \frac{\omega^{(6,6)}}{3^{1/2}} \right) \frac{\sigma^{(6)}}{1 + q} \\
 & + \frac{1}{2^{1/2}} (\tilde{\xi}^{(2)} \omega^{(2,2)} \sigma^{(2)} + \tilde{\xi}^{(5)} \omega^{(5,5)} \sigma^{(5)}) \\
 & \left. + \frac{1}{2^{1/2}} (\tilde{\xi}^{(3)} \omega^{(3,3)} \sigma^{(3)} + \tilde{\xi}^{(4)} \omega^{(4,4)} \sigma^{(4)}) \right] \tag{B 1 a}
 \end{aligned}$$

and

$$\begin{aligned}
 & \sum_{l \text{ class}} k_l^2 \hat{b}_m^l \hat{b}_n^l b_{mn}^{(\beta)} \\
 \approx N_{\text{d}} Z_0 \tilde{Q} & \left[\hat{Q}^{(\beta)} + \left([\hat{Q}^{(\beta)} - (3 + 2q)\hat{\psi}^{(\beta)}] \frac{\omega^{(1,1)}}{6^{1/2}} + (\hat{Q}^{(\beta)} + q\hat{\psi}^{(\beta)}) \frac{\omega^{(6,1)}}{3^{1/2}} \right) \frac{\sigma^{(1)}}{1 + q} \right. \\
 & + \left([\hat{Q}^{(\beta)} - (3 + 2q)\hat{\psi}^{(\beta)}] \frac{\omega^{(1,6)}}{6^{1/2}} + (\hat{Q}^{(\beta)} + q\hat{\psi}^{(\beta)}) \frac{\omega^{(6,6)}}{3^{1/2}} \right) \frac{\sigma^{(6)}}{1 + q} \\
 & + \frac{1}{2^{1/2}} (\hat{\xi}^{(\beta,2)} \omega^{(2,2)} \sigma^{(2)} + \hat{\xi}^{(\beta,5)} \omega^{(5,5)} \sigma^{(5)}) \\
 & \left. + \frac{1}{2^{1/2}} (\hat{\xi}^{(\beta,3)} \omega^{(3,3)} \sigma^{(3)} + \hat{\xi}^{(\beta,4)} \omega^{(4,4)} \sigma^{(4)}) \right]. \tag{B 1 b}
 \end{aligned}$$

Here N_{d} is a normalization factor such that $N_{\text{d}} \rho_{\text{d}}^{\lambda_l, \phi_l}$ is the line density of the l -class dislocation with line direction defined by the Euler angles (λ_l, ϕ_l) . If $\rho_{\text{d}}^{\lambda_l, \phi_l}$ is given by the line densities, then $N_{\text{d}} = 1$. However, if $\rho_{\text{d}}^{\lambda_l, \phi_l}$ is given in density fractions, then N_{d} is the total line density. The other parameters in equations (B 1) are defined as follows:

$$\begin{aligned}
 \tilde{Q} &= \sum_{l \text{ class}} \sum_{\lambda_l, \phi_l} \rho_{\text{d}}^{\lambda_l, \phi_l} (1 + q \cos^2 \lambda_l)^{1/2}, \\
 \tilde{\psi} &= \frac{1}{\tilde{Q}} \sum_{l \text{ class}} \sum_{\lambda_l, \phi_l} \frac{\rho_{\text{d}}^{\lambda_l, \phi_l} \sin^2 \lambda_l}{2(1 + q \cos^2 \lambda_l)^{1/2}}, \\
 \tilde{\xi}^{(2)} &= \frac{1}{\tilde{Q}(1 + q)} \sum_{l \text{ class}} \sum_{\lambda_l, \phi_l} \frac{\rho_{\text{d}}^{\lambda_l, \phi_l} \cos(2\phi_l) \sin^2 \lambda_l}{2(1 + q \cos^2 \lambda_l)^{1/2}}, \\
 \tilde{\xi}^{(5)} &= \frac{-1}{\tilde{Q}(1 + q)} \sum_{l \text{ class}} \sum_{\lambda_l, \phi_l} \frac{\rho_{\text{d}}^{\lambda_l, \phi_l} \sin(2\phi_l) \sin^2 \lambda_l}{2(1 + q \cos^2 \lambda_l)^{1/2}},
 \end{aligned}$$

$$\begin{aligned}
 \tilde{\xi}^{(3)} &= \frac{-1}{\tilde{Q}} \sum_{l \text{ class}} \sum_{\lambda_l, \phi_l} \frac{\rho_d^{\lambda_l, \phi_l} \cos \phi_l \sin(2\lambda_l)}{2(1+q \cos^2 \lambda_l)^{1/2}}, \\
 \tilde{\xi}^{(4)} &= \frac{-1}{\tilde{Q}} \sum_{l \text{ class}} \sum_{\lambda_l, \phi_l} \frac{\rho_d^{\lambda_l, \phi_l} \sin \phi_l \sin(2\lambda_l)}{2(1+q \cos^2 \lambda_l)^{1/2}}, \\
 \hat{Q}^{(\beta)} &= \frac{1}{\tilde{Q}} \sum_{l \text{ class}} \sum_{\lambda_l, \phi_l} \rho_d^{\lambda_l, \phi_l} (1+q \cos^2 \lambda_l)^{1/2} \hat{b}_m^l \hat{b}_n^l b_{mn}^{(\beta)}, \\
 \hat{\psi}^{(\beta)} &= \frac{1}{\tilde{Q}} \sum_{l \text{ class}} \sum_{\lambda_l, \phi_l} \frac{\rho_d^{\lambda_l, \phi_l} \sin^2 \lambda_l}{2(1+q \cos^2 \lambda_l)^{1/2}} \hat{b}_m^l \hat{b}_n^l b_{mn}^{(\beta)}, \\
 \hat{\xi}^{(\beta,2)} &= \frac{1}{\tilde{Q}(1+q)} \sum_{l \text{ class}} \sum_{\lambda_l, \phi_l} \frac{\rho_d^{\lambda_l, \phi_l} \cos(2\phi_l) \sin^2 \lambda_l}{2(1+q \cos^2 \lambda_l)^{1/2}} \hat{b}_m^l \hat{b}_n^l b_{mn}^{(\beta)}, \\
 \hat{\xi}^{(\beta,5)} &= \frac{-1}{\tilde{Q}(1+q)} \sum_{l \text{ class}} \sum_{\lambda_l, \phi_l} \frac{\rho_d^{\lambda_l, \phi_l} \sin(2\phi_l) \sin^2 \lambda_l}{2(1+q \cos^2 \lambda_l)^{1/2}} \hat{b}_m^l \hat{b}_n^l b_{mn}^{(\beta)}, \\
 \hat{\xi}^{(\beta,3)} &= \frac{-1}{\tilde{Q}} \sum_{l \text{ class}} \sum_{\lambda_l, \phi_l} \frac{\rho_d^{\lambda_l, \phi_l} \cos \phi_l \sin(2\lambda_l)}{2(1+q \cos^2 \lambda_l)^{1/2}} \hat{b}_m^l \hat{b}_n^l b_{mn}^{(\beta)}, \\
 \hat{\xi}^{(\beta,4)} &= \frac{-1}{\tilde{Q}} \sum_{l \text{ class}} \sum_{\lambda_l, \phi_l} \frac{\rho_d^{\lambda_l, \phi_l} \sin \phi_l \sin(2\lambda_l)}{2(1+q \cos^2 \lambda_l)^{1/2}} \hat{b}_m^l \hat{b}_n^l b_{mn}^{(\beta)}. \tag{B 2}
 \end{aligned}$$

All the parameters defined above depend mainly on the microstructure of the metal. Their dependence on point-defect properties is only through q . Therefore, for cubic metals, when $q = 0$, they do not have any point-defect dependence. From equations (B 1), we can write

$$\begin{aligned}
 \frac{\sum_{l \text{ class}} k_I^2 \hat{b}_m^l \hat{b}_n^l b_{mn}^{(\beta)}}{k_T^2} &\approx \left[\hat{Q}^{(\beta)} + (\hat{\psi}^{(\beta)} - \hat{Q}^{(\beta)} \tilde{\psi}) \left(\frac{q}{1+q} \frac{\omega^{(6,1)}}{3^{1/2}} - \frac{3+2q}{1+q} \frac{\omega^{(1,1)}}{6^{1/2}} \right) \right]^{(1)} \\
 &+ (\hat{\psi}^{(\beta)} - \hat{Q}^{(\beta)} \tilde{\psi}) \left(\frac{q}{1+q} \frac{\omega^{(6,6)}}{3^{1/2}} - \frac{3+2q}{1+q} \frac{\omega^{(1,6)}}{6^{1/2}} \right) \right]^{(6)} \\
 &+ (\hat{\xi}^{(\beta,2)} - \hat{Q}^{(\beta)} \tilde{\xi}^{(2)}) \frac{\omega^{(2,2)}}{2^{1/2}} \sigma^{(2)} + (\hat{\xi}^{(\beta,2)} - \hat{Q}^{(\beta)} \tilde{\xi}^{(5)}) \frac{\omega^{(5,5)}}{2^{1/2}} \sigma^{(5)} \\
 &+ (\hat{\xi}^{(\beta,3)} - \hat{Q}^{(\beta)} \tilde{\xi}^{(3)}) \frac{\omega^{(3,3)}}{2^{1/2}} \sigma^{(3)} + (\hat{\xi}^{(\beta,4)} - \hat{Q}^{(\beta)} \tilde{\xi}^{(4)}) \frac{\omega^{(4,4)}}{2^{1/2}} \sigma^{(4)} \Big].
 \end{aligned}$$

From equation (11) the strain rate is given by

$$\dot{\epsilon}^{(\beta)} = G \left(\dot{g}^{(\beta)} + \sum_{\beta'} K^{(\beta, \beta')} \sigma^{(\beta')} \right) \tag{B 3}$$

where

$$\dot{g}^{(\beta)} = \hat{Q}_I^{(\beta)} - \hat{Q}_V^{(\beta)},$$

$$\mathbf{K}^{(\beta, \beta')} \left\{ \begin{array}{l} = \left[(\hat{\psi}_i^{(\beta)} - \hat{Q}_i^{(\beta)} \tilde{\psi}_i) \left(\frac{q_i}{1+q_i} \frac{\omega_i^{(6, \beta')}}{3^{1/2}} - \frac{3+2q_i}{1+q_i} \frac{\omega_i^{(1, \beta')}}{6^{1/2}} \right) \right. \\ \left. - (\hat{\psi}_v^{(\beta)} - \hat{Q}_v^{(\beta)} \tilde{\psi}_v) \left(\frac{q_v}{1+q_v} \frac{\omega_v^{(6, \beta')}}{3^{1/2}} - \frac{3+2q_v}{1+q_v} \frac{\omega_v^{(1, \beta')}}{6^{1/2}} \right) \right] \text{ for } \beta' = 1 \text{ or } 6, \\ = (\hat{\xi}_i^{(\beta, \beta')} - \hat{Q}_i^{(\beta)} \tilde{\xi}_i^{(\beta')}) \frac{\omega_i^{(\beta')}}{2^{1/2}} - (\hat{\xi}_v^{(\beta, \beta')} - \hat{Q}_v^{(\beta)} \tilde{\xi}_v^{(\beta')}) \frac{\omega_v^{(\beta')}}{2^{1/2}} \text{ for } \beta' = 2, 3, 4 \text{ or } 5. \end{array} \right.$$

ACKNOWLEDGEMENTS

The authors wish to acknowledge funding support from Hong Kong Research Grant Council (PolyU 5123/98E) (C.H.W) and CANDU Owners Group (C.B.S.).

REFERENCES

- CHRISTODOULOU, N., CAUSEY, A. R., WOO, C. N., TOMÉ, C. N., KLASSEN, R. J., and HOLT, R. A., 1993, ASTM Special Technical Publication 1175 (Philadelphia, Pennsylvania: American Society for Testing and Materials), pp. 1111–1128.
- DEDERICHS, P. H., and SCHROEDER, K., 1978, *Phys. Rev. B*, **17**, 2524.
- FERNÁNDEZ, J. R., MONTI, A. M., SARCE, A., and SMETNIANSKY-DE GRANDE, N., 1994, *J. nucl. Mater.*, **210**, 282.
- FISCHER, E. S., and RENKEN, C. J., 1964, *Phys. Rev. A*, **135**, 482.
- FLYNN, C. P., 1972, *Point Defects and Diffusion* (Oxford: Clarendon).
- HOLT, R. A., 1988, *J. nucl. Mater.*, **159**, 310.
- LEIBFRIED, G., and BREUER, N., 1978, *Point Defects in Metals I: Introduction to the Theory* (Berlin: Springer).
- MONTI, A. M., 1991, *Phys. Stat. sol. (b)* **168**, 49.
- SAVINO, E. J., 1977, *Phil. Mag.*, **36**, 323.
- SAVINO, E. J., and SMETNIANSKY-DE GRANDE, N., 1987, *Phys. Rev. B*, **35**, 6064.
- SKINNER, B. C., and WOO, C. H., 1984, *Phys. Rev. B*, **30**, 3084.
- SMETNIANSKY-DE GRANDE, N., TOMÉ, C. N., and SAVINO, E. J., 1991, *Phys. Stat. sol. (b)*, **167**, 477.
- WOO, C. H., 1984, *J. nucl. Mater.*, **120**, 55; 1987a, ASTM Special Technical Publication 955 (Philadelphia, Pennsylvania: American Society for Testing and Materials), p. 70; 1987b, *Materials for Nuclear Reactor Core Applications*, Vol. 1 (London: British Nuclear Energy Society), p. 65; 1988, *J. nucl. Mater.*, **159**, 237; 1995, *ibid.*, **225**, 8; 1998, *Radiat. Effects Defects Solids*, **144**, 145.
- WOO, C. H., and GARNER, F. A., 1992, *J. nucl. Mater.*, **191–194**, 1309; 1996, *ibid.*, **233–237**, 974; 1999, *ibid.*, **271–272**, 78.
- WOO, C. H., GARNER, F. A., and HOLT, R. A., 1993, ASTM Special Technical Publication 1175 (Philadelphia, Pennsylvania: American Society for Testing and Materials), p. 27.
- WOO, C. H., and GOESELE, U., 1983, *J. nucl. Mater.*, **119**, 219.
- WOO, C. H., HOLT, R. A., and GRIFFITHS, M., 1992, *Materials Modelling: From Theory to Technology* (Bristol: Institute of Physics), pp. 55–60.
- WOO, C. H., and SAVINO, E. J., 1983, *J. nucl. Mater.*, **116**, 17.
- WOO, C. H., and SINGH, B. N., 1992, *Phil. Mag. A*, **65**, 889.